

Competing interactions and complex magnetism at SrRuO₃/SrMnO₃ interfaces

Y. Choi,^{1,a)} Y. C. Tseng,^{1,2} D. Haskel,¹ D. E. Brown,³ D. Danaher,³ and O. Chmaissem^{3,4}

¹Advanced Photon Source, Argonne National Laboratory, Argonne, Illinois 60439, USA

²Department of Materials Science and Engineering, Northwestern University, Evanston, Illinois 60439, USA

³Institute for NanoScience, Engineering, and Technology, Physics Department, Northern Illinois University, DeKalb, Illinois 60115, USA

⁴Materials Science Division, Argonne National Laboratory, Argonne, Illinois 60439, USA

(Received 4 September 2008; accepted 14 October 2008; published online 12 November 2008)

The coupled interfacial Mn and Ru spin configurations in a SrRuO₃(SRO)/SrMnO₃(SMO) superlattice are investigated with x-ray resonant techniques. With an out-of-plane applied field H , a net Mn moment is induced opposite to (along) H below (above) SRO Curie temperature T_C , due to changes in interfacial antiferromagnetic Ru–Mn coupling. In comparison with the Mn moment induced along an out-of-plane field below T_C , the Mn moment induced along an in-plane field is five (three) times smaller below (above) T_C , due to frustration in the Ru–Mn coupling. Despite its in-plane anisotropy, the G-type antiferromagnetic SMO favors out-of-plane over in-plane canting of Mn moments. © 2008 American Institute of Physics. [DOI: 10.1063/1.3013333]

Recent advances in pulsed layer deposition (PLD) techniques have allowed the growth of artificial superlattices with nearly atomically flat interfaces.¹ The properties of the interfacial regions where dissimilar materials are forced to coexist differ significantly from the bulk providing a playground for the development of materials with tailored properties. Examples of important phenomena include exchange bias at the antiferromagnetic (AFM)-ferromagnetic (FM) interface and spin-dependent scattering/tunneling magnetoresistance effects. Electronic spins at the interfaces of epitaxial heterostructures are subject to competing interactions arising from magnetocrystalline anisotropy, intralayer and interlayer exchange coupling, and applied magnetic fields. The recent advances in x-ray magnetic circular dichroism (XMCD) and x-ray resonant magnetic scattering (XRMS) techniques provide unique capabilities for the studies of element-specific interfacial spin configurations, key to understanding the complex magnetic behavior in confined heterostructures.

Perovskite SrRuO₃ (SRO) and SrMnO₃ (SMO) materials possess interesting electronic and magnetic properties. Their small lattice mismatch allows good structural coherence and high quality interfaces. In the bulk, SRO is a ferromagnet with a Curie temperature T_C of ~ 163 K (Refs. 2–4) and strong magnetocrystalline anisotropy, whereas SMO is a G-type antiferromagnet with a Néel temperature T_N of ~ 260 K.⁵ In this work, we investigate the roles of anisotropy, interfacial coupling, and magnetic fields in inducing Mn spin canting in SRO/SMO superlattices for $T < T_C < T_N$ and $T_C < T < T_N$, as well as in inducing net interfacial Ru magnetization for $T_C < T < T_N$ [i.e., above T_C (SRO)]. Our results show that the presence or absence of Ru magnetic ordering has dramatic effects on the induced magnetism in the SMO layers. The combination of XMCD and XRMS provides valuable insight into the interfacial magnetic structure of SRO/SMO beyond the capabilities of bulk-sensitive techniques.

A single-crystalline (SRO/SMO)₁₉ superlattice film was grown on a SrTiO₃(100) substrate by PLD as detailed in Ref. 6. The SRO and SMO layers are 10 and 2 unit cell thick, respectively, and the film was capped with an extra SRO layer. Due to the small layer thickness of SMO, the Mn magnetic response is most sensitive to the interfacial coupling with the adjacent SRO layers. As grown on SrTiO₃, SRO and SMO layers exhibit out-of-plane and in-plane anisotropies, respectively. Superconducting quantum interference device magnetization data taken at 50 K [$T < T_C$ (SRO) $< T_N$ (SMO)] indicate the out-of-plane direction as the easy axis of the superlattice in agreement with the dominant contributions of the thicker FM SRO layers.⁷ With the field along the hard axis (in plane) the Ru moment reaches $\sim 60\%$ and $\sim 70\%$ of its saturation value at 10 and 40 kOe, respectively. Element-specific XMCD and XRMS magnetic characterizations of SRO and SMO layers were carried out using circularly polarized synchrotron radiation at beamline 4ID-C of the Advanced Photon Source of Argonne National Laboratory with x-ray energies tuned near the Mn L and Ru L absorption edges. Out-of-plane XMCD data were collected in normal incidence using total electron yield detection mode to detect the out-of-plane component of the magnetization. In-plane XRMS measurements were performed at grazing incidence using specularly reflected x rays probing the in-plane magnetization component in scattering plane.^{8,9} An external magnetic field H was applied parallel to the incident x-ray wave vector \mathbf{k} . XMCD and XRMS data were collected at a fixed incident angle θ by recording the helicity-dependent absorbed and scattered intensities I^+ and I^- as a function of x-ray incident energy. Hereafter, we define the XMCD and XRMS asymmetry ratios as $(I^+ - I^-)/(I^+ + I^-)$.

Based on results from similarly structured oxide films,^{7,10–14} the Mn–Ru coupling is expected to be AFM. In a previous study, we measured a surprisingly large out-of-plane ($\theta = 90^\circ$) Mn-XMCD signal at 50 K and low magnetic fields that nearly vanishes at ± 40 kOe [Fig. 1(a)].⁷ At low fields, the combined effects of interfacial Mn–Ru AFM cou-

^{a)}Present address: GSECARS, University of Chicago, Chicago, Illinois 60637, USA. Electronic mail: choi@cars.uchicago.edu.

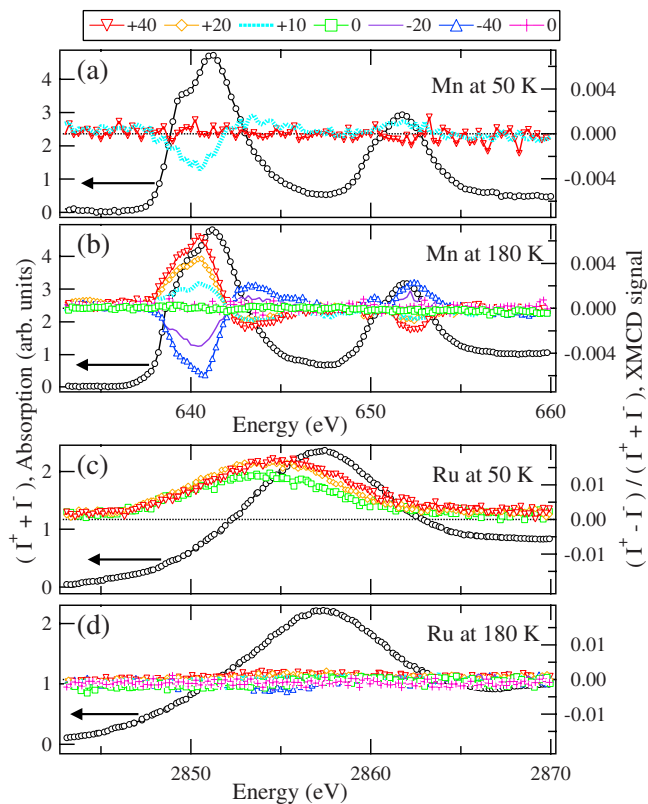


FIG. 1. (Color online) Magnetic field (in kOe) dependence of out-of-plane ($\theta=90^\circ$) XMCD signals. Mn $L_{2,3}$ edges at (a) 50 and (b) 180 K. Ru L_3 edge at (c) 50 K and (d) 180 K.

pling and SRO out-of-plane anisotropy force the Mn moments in SMO to cant against the direction of the applied field and Ru moments [see opposite signs of XMCD signals for Mn and Ru in Figs. 1(a) and 1(c)]. At higher fields, the (negative) out-of-plane component is reduced to minimize the Zeeman energy.⁷

To further evaluate the effects of out-of-plane magnetic ordering in the SRO layers on the magnetic response in the SMO layers, Mn- and Ru-XMCD measurements were carried out at 180 K ($T_C < 180 \text{ K} < T_N$) as shown in Figs. 1(b) and 1(d). As expected above T_C , the absence of SRO magnetization and its out-of-plane anisotropy results in no measurable out-of-plane Ru-XMCD signal, as shown in Fig. 1(d). Hence, with no Mn–Ru coupling, the starting zero-field spin structure in the SMO layers corresponds to a typical planar G-type configuration in which the Mn moments would cant in the same direction as the applied magnetic field (e.g., opposite to the direction observed at 50 K), as seen in Figs. 1(a) and 1(b). The sketch in the left panel of Fig. 2 shows how the presence (absence) of Ru magnetic ordering together with AFM Mn–Ru exchange coupling at the SRO/SMO interfaces below (above) T_C is responsible for these differences. As shown in Fig. 1(b), the Mn-XMCD signal is zero at $H=0$ kOe and returns to zero after the application and removal of a reversing field of -40 kOe. This behavior clearly indicates that the induced net Mn moment is solely due to canting of the AFM Mn spin structure and not due to the presence of isolated FM domains.

In-plane ($\theta=5.1^\circ$) Mn- and Ru-XRMS signals measured at 180 K are shown in Figs. 3(a) and 3(b), respectively.¹⁵ The Mn-XRMS signal is field dependent and increases with increasing magnetic fields. As with the out-of-plane case, this

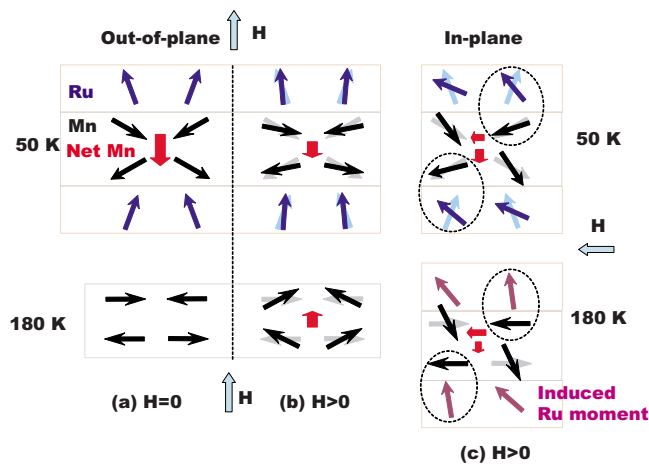


FIG. 2. (Color online) Schematics for the in-plane and out-of-plane interfacial spin configurations at 50 and 180 K.

XRMS signal is zero at $H=0$ kOe and returns to zero after the application and removal of a reversing field of -10 kOe, in agreement with a zero-field collinear in-plane Mn AFM structure and field-dependent canted Mn AFM structures. In contrast to the out-of-plane results, a significant in-plane Ru-XRMS signal is observed, above T_C , increasing with H [Fig. 3(b)]. This induced Ru moment is not of paramagnetic origin as it has not been observed in the out-of-plane XMCD measurements, which probe the entire SRO layers. The high sensitivity of XRMS to interfacial magnetization indicates that the Ru moment is rather induced through Mn–Ru AFM interfacial coupling and that it primarily resides at the interfaces.

In order to quantitatively compare the in-plane and out-of-plane canted Mn moments, Mn-XRMS data were fit using Parratt's recursive formalism¹⁶ adapted to describe the charge-magnetic interference scattering probed in the XRMS measurements.¹⁷ Scalar imaginary parts f'' and fm'' of charge and magnetic resonant scattering factors were directly extracted from the measured absorption spectra in Fig. 1(a) while the real parts f' and fm' were obtained through a differential Kramers–Kronig transformation.¹⁸ Tabulated scattering factors¹⁹ were used for the nonresonant elements. The magnitude of the out-of-plane net Mn moment at $H=10$ kOe and $T=50$ K defined as ΔM serves as an arbitrary

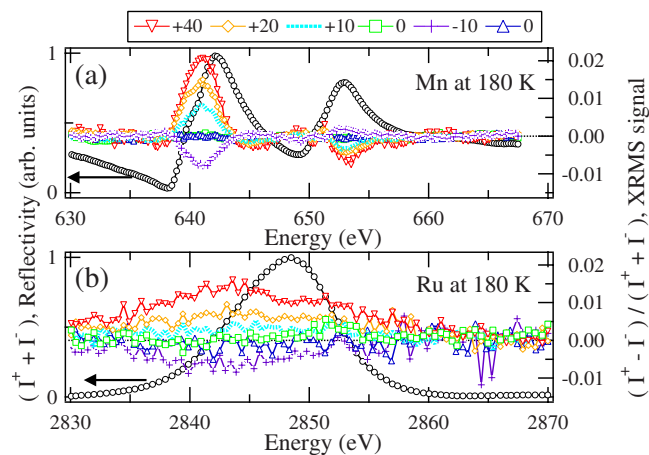


FIG. 3. (Color online) Magnetic field (in kOe) dependence of in-plane ($\theta=5.1^\circ$) XRMS signals. (a) Mn $L_{2,3}$ edges at 180 K. (b) Ru L_3 edge at 180 K.

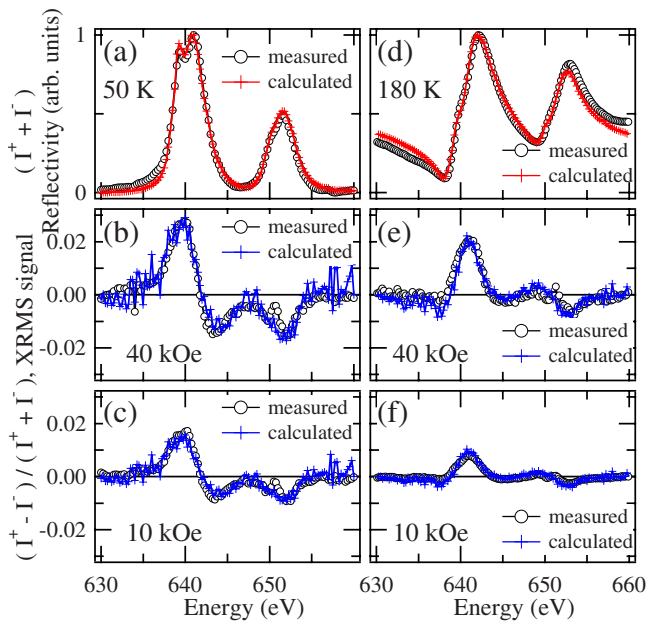


FIG. 4. (Color online) Measured and calculated XRMS reflectivity curves near the Mn $L_{2,3}$ edges. [(a)–(c)] At 50 K, with $\theta=10.8^\circ$. [(d)–(f)] At 180 K, with $\theta=5.1^\circ$.

reference against which the refined in-plane Mn moments are compared. Figure 4 shows in-plane XRMS data and fits for 50 K ($\theta=10.8^\circ$) and 180 K ($\theta=5.1^\circ$), respectively. Spin-independent reflectivity ($I^+ + I^-$) is only sensitive to the chemical structure and was calculated using the nominal structure of the superlattice, as shown in Figs. 4(a) and 4(d). Since the XRMS signal depends on both the chemical and magnetic structures, the fits were performed using the nominal structural parameters and varying the magnitude of the in-plane net Mn moment along H , assuming all SMO layers are identical and uniformly magnetized within each layer. As shown in Fig. 4, excellent fits to the data are obtained with magnetic scattering factors fm' and fm'' scaled down by 0.33 and 0.18 (at 50 K) or 0.6 and 0.28 (at 180 K) for 40 and 10 kOe, respectively. These refined scaling factors indicate that at these fields and temperatures the in-plane net Mn moments are only a fraction of the out-of-plane Mn moment ΔM at 10 kOe and 50 K.

The relative size of the canted Mn moment at the various temperatures and applied field directions is shown schematically in Fig. 2. The asymmetric canting of the Mn moments in response to an in-plane applied magnetic field results in a small in-plane FM component in the direction of the applied field. However, when the SRO is FM ordered in plane, the emergence of Mn–Ru AFM interfacial ordering is not completely possible in the presence of Mn–Mn AFM interac-

tions, due to frustration in the interfacial Mn–Ru exchange coupling, which results in some suppression of the in-plane Mn induced moment (see circled Mn–Ru interactions in Fig. 2). This frustration is partly relieved above T_C where the field-induced net in-plane Mn moment increases. Thus, in the presence of Mn–Ru exchange coupling the SMO/SRO interface favors out-of-plane canting versus in-plane canting of Mn and Ru moments. The results provide insights into the interdependent effects of anisotropy, interfacial coupling, and frustration on the canted magnetic structure of nominal AFM-SMO/FM-SRO layers in this exchange-coupled complex oxide superlattice system.

The work at Argonne National Laboratory was supported by U.S. Department of Energy, Office of Science, under Contract No. DE-AC02-06CH11357.

- ¹T. Venkatesan, X. D. Wu, A. Inam, and J. B. Wachtman, *Appl. Phys. Lett.* **52**, 1193 (1988).
- ²A. Callaghan, C. W. Moeller, and R. Ward, *Inorg. Chem.* **5**, 1572 (1966).
- ³A. Kanbayasi, *J. Phys. Soc. Jpn.* **41**, 1876 (1976).
- ⁴Y. Z. Yoo, O. Chmaissem, S. Kolesnik, A. Ullah, L. B. Lurio, D. E. Brown, J. Brady, B. Dabrowski, C. W. Kimball, M. Haji-Sheikh, and A. P. Genis, *Appl. Phys. Lett.* **89**, 124104 (2006).
- ⁵T. Takeda and S. Ohara, *J. Phys. Soc. Jpn.* **37**, 275 (1974).
- ⁶Y. Z. Yoo, O. Chmaissem, S. Kolesnik, B. Dabrowski, M. Maxwell, C. W. Kimball, L. McAnelly, M. Haji-Sheikh, and A. P. Genis, *J. Appl. Phys.* **97**, 103525 (2005).
- ⁷Y. Choi, Y. Z. Yoo, O. Chmaissem, A. Ullah, S. Kolesnik, C. W. Kimball, D. Haskel, J. S. Jiang, and S. D. Bader, *Appl. Phys. Lett.* **91**, 022503 (2007).
- ⁸J. P. Hannon, G. T. Trammell, M. Blume, and D. Gibbs, *Phys. Rev. Lett.* **61**, 1245 (1988).
- ⁹D. Haskel, G. Srajer, J. C. Lang, J. Pollmann, C. S. Nelson, J. S. Jiang, and S. D. Bader, *Phys. Rev. Lett.* **87**, 207201 (2001).
- ¹⁰F. Weigand, S. Gold, A. Schmid, J. Geissler, E. Goering, K. Dör, G. Krabbes, and K. Ruck, *Appl. Phys. Lett.* **81**, 2035 (2002).
- ¹¹H. Yamada, M. Kawasaki, and Y. Tokura, *Appl. Phys. Lett.* **86**, 192505 (2005).
- ¹²P. Padhan, W. Prellier, and R. C. Budhani, *Appl. Phys. Lett.* **88**, 192509 (2006).
- ¹³Z. H. Han, J. I. Budnick, W. A. Hines, B. Dabrowski, and T. Maxwell, *Appl. Phys. Lett.* **89**, 102501 (2006).
- ¹⁴K. Terai, K. Yoshii, Y. Takeda, S. I. Fujimori, Y. Saitoh, K. Ohwada, T. Inami, T. Okane, M. Arita, K. Shimada, H. Namatame, M. Taniguchi, K. Kobayashi, M. Kobayashi, and A. Fujimori, *Phys. Rev. B* **77**, 115128 (2008).
- ¹⁵While the superlattice is probed in whole at normal incidence (XMCD measurements), the XRMS measurements at 5.1° and 10.8° incident angles probe approximately 4 and 12 bilayers, respectively, as verified by simulations of electric field intensity profiles inside the multilayer.
- ¹⁶L. G. Parratt, *Phys. Rev.* **95**, 359 (1954).
- ¹⁷D. R. Lee, S. K. Sinha, D. Haskel, Y. Choi, J. C. Lang, S. A. Stepanov, and G. Srajer, *Phys. Rev. B* **68**, 224409 (2003).
- ¹⁸J. O. Cross, M. Newville, J. J. Rehr, L. B. Sorensen, C. E. Bouldin, G. Watson, T. Gouder, G. H. Lander, and M. I. Bell, *Phys. Rev. B* **58**, 11215 (1998).
- ¹⁹D. T. Cromer and D. Liberman, *J. Chem. Phys.* **53**, 1891 (1970).